EVALUATION OF THE UAH GOES INSOLATION PRODUCT THROUGH COMPARISON WITH PYRANOMETER MEASUREMENTS AND ANALYSIS DATASETS

Peiyang Cheng *, Arastoo Pour-Biazar, Richard McNider, and John Mecikalski

Department of Atmospheric Sciences, University of Alabama in Huntsville, Huntsville, Alabama

Abstract

A high-resolution measurement of solar energy is anticipated by various climatological and agricultural researches and applications. However, the existing pyranometer network is not dense enough to meet the requirement. The University of Alabama in Huntsville (UAH) has started to establish an archive of surface insolation based on a simple physical model using Geostationary Operational Environmental Satellite (GOES) visible-band images to provide high-resolution insolation estimates over large domains. While this dataset has been used in the previous air quality studies with limited evaluation, it is necessary to conduct a rigorous evaluation to validate the retrieval and to elucidate limitations of the physical model. In this study, the UAH insolation product will be compared to pyranometer data to quantify the degree of agreement. The Rapid Refresh (RAP) analysis dataset will also be evaluated using the UAH insolation product with respect to surface radiation budgets. Results have indicated that the UAH insolation product compares well with pyranometer data under clear-sky conditions; but for cloudy skies, the spatial scale and transient nature of clouds makes the comparison difficult. Besides, the product performs well for all seasons in the warm regions (e.g. the Southern U.S.), but has shown significant underestimations during cold seasons in regions with cold climate. Snow cover is thought to be one of the causes, but the minimum brightness detection module in the retrieval system may also fail, which requires further investigations.

1. INTRODUCTION

As a substantial component of surface energy budget, solar radiation plays an important role in land surface-atmosphere interaction (Tarpley 1979; Gautier et al. 1980; Li et al. 1995; Otkin et al. 2005; Diak 2017). Instantaneous solar irradiance at the Earth's surface has been measured through ground-based pyranometers located at various weather stations and agricultural experiment stations for decades. However, the existing pyranometer networks cannot provide high-resolution solar radiation information for meteorological studies due to their limited density and non-uniform distribution (Li et al. 1995; Otkin et al. 2005). To obtain surface insolation data across the continental United States (CONUS), techniques using geostationary satellite images, such as images from Geostationary Operational Environmental Satellite (GOES), have been developed in the last few decades to provide large-scale high-resolution insolation retrieval (Schmetz 1989; Pinker et al. 1995; Diak et al. 2004; Otkin et al. 2005). These products typically have grids much finer than pyranometer networks, and can be applied to a variety of studies (Gautier et al. 1980; Otkin et al. 2005; Mecikalski et al. 2011; Diak 2017).

Generally, the retrieval techniques fall into two basic categories (Schmetz 1989). One develops empirical relationships between satellite estimates and pyranometer measurements. For example, Tarpley (1979) applied a statistical model to estimate the surface insolation. However, statistical models typically require observations from well-calibrated pyranometers to periodically adjust regression coefficients. Another category uses physical models to simulate physical processes in the atmosphere, which allows potential improvements of the model (Schmetz 1989; Otkin et al. 2005; Diak 2017). Gautier et al. (1980) developed a simple physical model to estimate solar radiation at the surface using GOES data with the highest spatial resolution. In this model, cloud effects were treated as continuous to better represent their modifications to solar radiation. Diak and Gautier (1983) further improved this model through modifying the existing physics and introducing more physical processes.

Later, more physical models using GOES data have been developed to estimate surface insolation. The University of Wisconsin-Madison is operating an insolation system based on a simple atmospheric radiative transfer (RT) model by Gautier et al. (1980) and Diak and Gautier (1983) (hereafter the Diak's model) with some modifications as summarized in Diak (2017). The National Oceanic and Atmospheric Administration (NOAA) has an operational product called Global Solar Insolation Project (GSIP), which retrieves global horizontal irradiance (GHI) using GOES visible and infrared channel imagery (Habte et al. 2012, 2013). The Short-term Prediction Research and Transition Center (SPoRT) at National Aeronautics and Space Administration's (NASA's) Marshall Space Flight Center in Huntsville is currently operating GOES Product Generation System (GPGS) to generate near real-time meteorological data products, including the surface insolation, from GOES-East Imager and Sounder measurements (Haines et al. 2004).

* *Corresponding author address*: Peiyang Cheng, University of Alabama in Huntsville, Atmospheric Science Department, Huntsville, AL, 35899; e-mail: peiyang.cheng@nsstc.uah.edu.

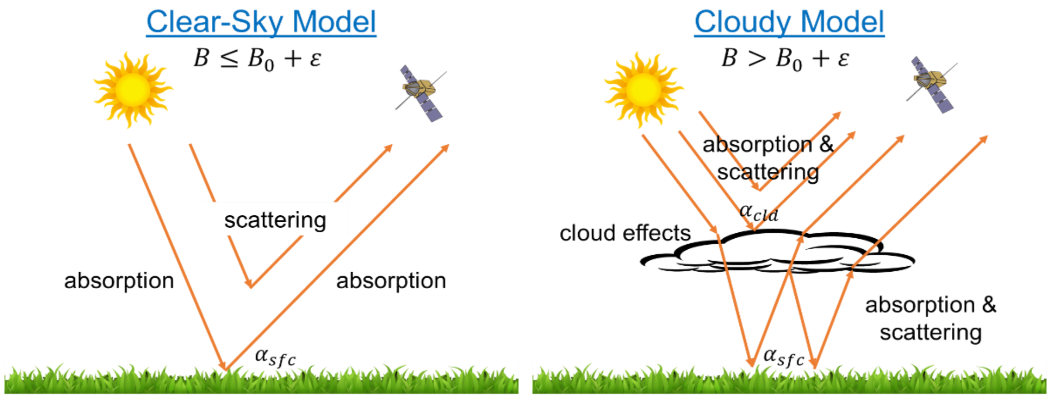

Fig. 1. Sketch of Diak's physical model for clear-sky (left panel) and cloudy conditions (right panel). B refers to the brightness obtained from GOES visible channel images, while B_0 refers to the brightness threshold for clear-sky conditions; ε is a small tolerance for clear-sky/cloudy decision. α_{sfc} and α_{cld} indicate the surface and cloud albedos, respectively.

Although studies have shown that high-resolution satellite-based insolation estimates have comparable data quality to the pyranometer measurements (Schmetz 1989; Pinker et al. 1995), these physical models still tend to over- or under-estimate surface insolation over certain regions or under certain conditions (Podlasly and Berger 2002; Jacobs et al. 2002; Habte et al. 2013).

Recently, the University of Alabama in Huntsville (UAH) has been archiving GPGS products, and has made several refinements over the previous approach. The main goal of this study is to comprehensively evaluate the incorporated insolation product to find any sources of systematic biases in the retrieval system. Appropriate evaluation metrics are selected to quantify the degree of agreement between satellite retrieval and pyranometer measurements. Moreover, the UAH insolation product will be used to evaluate net shortwave radiation flux at the surface from selected analysis dataset to ascertain any systemic bias in the analyzed outputs with respect to the surface energy budget.

2. BACKGROUND

The UAH insolation product is defined on a Lambert Conformal Conic map projection with roughly 4km spatial resolution over the CONUS. The temporal resolution is corresponding to the GOES-East full disk scan, which operates hourly on each 45-min-past-hour (Haines et al. 2004). The surface insolation (INS) retrieval algorithm is essentially an implementation of the Diak's model.

The insolation retrieval system consists of two separate models for clear-sky and cloudy conditions (Fig. 1). Once the procession unit receives new daytime (1145-2345 UTC) images, the image update module generates composite images storing minimum visible band brightness values at each pixel for the most recent 20 days. It is assumed that, for each pixel, there exists at least one cloud free image for each hour within any 20-day period. Therefore, by implementing the clear-sky model, surface albedo (ALB) can be calculated using the composite images. Next, a clear-sky/cloudy decision is made by comparing current visible-band brightness value B with the one stored in the composite image (B_0). It is assumed that the threshold of clear-sky brightness is the summation of B_0 and a small tolerance value ε (a certain percentage of B_0. If B is smaller than or equal to this threshold, then the pixel will be determined as clear-sky; while the opposite indicates cloudy condition.

For cloud free pixels, the clear-sky model is used to calculate INS, which includes bulk parameterizations for water vapor absorption (Paltridge 1973), Rayleigh scattering (Coulson 1959), and ozone absorption (Lacis and Hansen 1974). Other processes of less importance (e.g., Mie scattering and gaseous absorption) are also parameterized to optimize the model. While for cloudy pixels, the cloud albedo (CLDALB) has to be calculated based on the ALB, the radiation received by satellite sensor, and the knowledge of absorption and scattering processes within the earth-atmosphere column. Finally, we can obtain the INS under cloudy conditions after implementing the cloudy model.

3. DATA

The pyranometer data used in this study come from the Surface Radiation Budget Network (SURFRAD) (Augustine et al. 2000, 2005) and the U.S. Climate Reference Network (USCRN) (Diamond et al. 2013). The SURFRAD provides surface radiation measurements at seven stations with diverse climatic conditions. The data are quality controlled and processed into daily files with one-minute temporal resolution. While the USCRN is a systematic and sustained network of climate monitoring stations which contains more than 100 sites across the CONUS. The recorded surface solar radiation data are averaged into 5-minute values.

Furthermore, net shortwave radiation flux at the surface can be derived from different models, for example, the North American Regional Reanalysis (NARR) and the Rapid Refresh (RAP). The NARR is a high resolution (approximately 32km) combined model and assimilated dataset offers 3-hourly composites for the North American domain (Mesinger et al. 2006), while the RAP is an hourly-updated assimilation and model forecast system provides data on a 13-km resolution horizontal grid (Benjamin et al. 2016). For better spatial and temporal representation of model insolation, the RAP analysis dataset is utilized on a priority basis. The model outputs will be examined using the UAH insolation product with respect to the surface energy budget.

4. METHODOLOGY

4.1. *Evaluation Metrics*

Commonly used statistical indicators for model performance evaluation and their advantages and disadvantages have been discussed in numerous studies (e.g., Ali and Abustan 2014; Simon et al. 2012). Different types of model performance metrics, as defined in Table 1, were used to describe the degree of agreement between the UAH insolation product and pyranometer data. Simple linear regression (Eq. 1) is also used to illustrate the trend and bias in the insolation retrieval.

$$\hat{R} = \alpha + \beta O, \tag{1}$$

where the coefficients for linear relationships are

$$\beta = \frac{\sum[(O_i - \bar{O})(R_i - \bar{R})]}{\sum(O_i - \bar{O})^2}, \tag{2}$$

$$\alpha = \bar{R} - b\bar{O}. \tag{3}$$

Here, R and O represent the insolation estimate and observation: R_i and O_i indicate specific data points; $\bar{R}$ and $\bar{O}$ show the averaged values; while $\hat{R}$ is the estimate of insolation retrieval.

4.2. *Comparison with Pyranometer Measurements*

Considering data availability and data gaps, this study has focused on a one-year period from March 1st, 2013 to February 28th, 2014. The satellite retrievals and pyranometer measurements were compared for both hourly and daily cumulative insolation. The comparison was carried out on a seasonal basis, to show any seasonal variations in the performance of the UAH insolation product. Since the time references of two datasets are different, the pyranometer data were averaged over each hour to make sure the time stamps coincide with GOES images. Also, to compensate for the effects of transient clouds and aerosol plumes, satellite estimates were not picked directly from the pixel where pyranometer site is located. They were selected as the best-fit values from the surrounding 3×3 box. Moreover, daily cumulative insolation is calculated by integrating hourly insolation with trapezoid rule. No interpolation was used to fill the data gaps.

Abbreviation	Evaluation Metric	Definition
MBE	Mean Bias Error	$MBE = \frac{1}{N}\sum(M_i - O_i)$
RMSE	Root Mean Square Error	$RMSE = \sqrt{\frac{1}{N}\sum(M_i - O_i)^2}$
R^2	Coefficient of Determination	$R^2 = \left(\frac{\sum[(M_i-\bar{M})\times(O_i-\bar{O})]}{\sqrt{\sum(M_i-\bar{M})^2\times\sum(O_i-\bar{O})^2}}\right)^2$

Table 1. Definitions of performance metrics.

4.3. *Comparison with Analysis Datasets*

To evaluate RAP analysis data, it is necessary to map the UAH insolation product onto RAP native grids since the spatial resolution of two datasets are different. This was done using EPA's Spatial Allocator tool (available at https://www.cmascenter.org/sa-tools/). A surface energy budget study will be carried out in the near future by comparing daily cumulative insolation of two datasets at each pixel.

5. UNCERTAINTIES

Some sources of uncertainty in pyranometer measurements and satellite estimates must be addressed since they can bring biases into our validation system.

Calibration uncertainty in pyranometers is one of the common issues, which is expected to be on the order of 5% of the mean insolation value (Augustine et al. 2000). A comparison of monthly averaged clear-sky insolation observation between SURFRAD and USCRN sites at Sioux Falls, SD for the month of July 2013 is shown in Figure 2. Reason for selecting this site is that the distance between two pyranometers is only about 100 feet. We can therefore assume that they were receiving the same amount of energy and are under the same cloud condition. Although we can find some daytime fluctuations, which were probably due to diurnal variations in the number of clear-sky samples, the plot has shown a good correlation between pyranometer measurements. The relative difference in clear-sky insolation was about 5% (50 out of 1000 W/m^2) near noon time, which implied the bias between instruments. Also, measurements can be affected by dust, insects, or transient clouds if they appeared in the viewing direction of sensor.

On the other hand, uncertainties in GOES insolation estimates are mainly due to satellite sensor degradation and image navigation error (Otkin et al. 2005; Diak 2017). The former issue can be corrected by post-launch calibration while the latter requires a precise navigation system.

Next, discrepancies in instrument working principles also introduce biases into our validation system. The

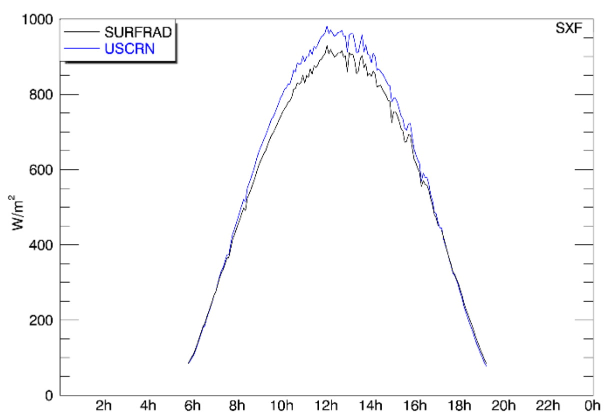

Fig. 2. Monthly averaged clear-sky insolation data measured from SURFRAD (black line) and USCRN (blue line) sites at Sioux Falls, SD for the month of July 2013.

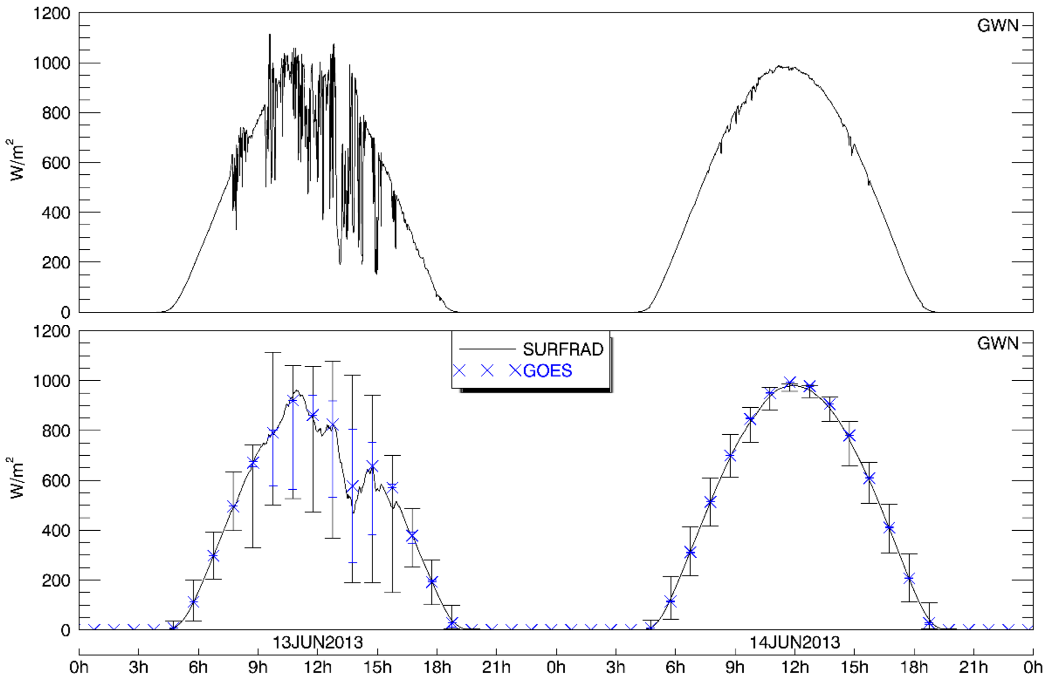

Fig. 3. A comparison of insolation plots from cloudy (June 13, 2013) and clear day (June 14, 2013) collected at SURFRAD Goodwin Creek, MS station. Top panel indicates raw insolation measurements while the black lines in bottom panel represented data after a running mean treatment. In the bottom panel, blue crosses indicate GOES best-fit values near the SURFRAD site, black and blue bars show ranges of hourly variations in pyranometer measurements and satellite estimates, respectively.

GOES Imager takes snapshots within a single narrow band over a small solid angle field of view. The retrieved insolation represents a spatial averaged value over a large area. However, pyranometer measures integrated hemispheric radiation continuously over total-solar-band at a single point. Therefore, space/time translation and spectrum transformation are required to make the datasets comparable (Gautier et al. 1980).

Furthermore, pyranometer measurements are highly variable in time when small scale broken clouds or aerosol plumes pass over the site. While these facts can also affect the UAH insolation retrieval, for example, a piece of cloud appears in a clear-sky region when the satellite is scanning. A comparison of insolation plots from cloudy and clear day collected at SURFRAD Good Creek, MS station is shown in Fig. 3. The 1-min raw data (top panel) has shown a strong fluctuation on June 13, 2013 due to clouds, but a smooth curve on the clear day (June 14, 2013). To compensate for the effects of broken clouds or aerosol plumes, as well as differences in viewing processes, SURFRAD data were averaged on an hourly basis (bottom panel). The existence of broken clouds has introduced large temporal variations in the measurement on the first day. This was reflected by the vertical bars showing hourly variation of the data. However, satellite retrieval under cloudy sky was still close to the mean measurements. On the other hand, the insolation can be reasonably estimated under clear air conditions. Moreover, most of the satellite-estimated values fall within one standard deviations of the mean measurements (not shown here), which has implied the confidence of our results.

6. RESULTS AND DISCUSSIONS

Seasonal comparisons of hourly and daily integrated insolation estimated from GOES-East visible channel images and measured from SURFRAD Goodwin Creek, MS and Sioux Falls, SD stations are presented in Figs. 4 and 5. The reason for selecting these two sites is that they have a warm and cold climate, respectively. Statistics indicated that their typical features can represent the other stations with warm or cold climates.

For hourly insolation comparison, Goodwin Creek station has shown low bias, high correlation ($R^2 \geq 0.98$) and small deviation from the best-fit lines for all seasons, indicating the satellite product can do well in the regions with warm climate (e.g. the Southern US). However, it showed a relatively poorer performance in cold climate regions, especially during the winter time with significant underestimations, as indicated by Sioux Falls station.

While for daily cumulative insolation comparison, the integrated values have reduced scattering features as the relative RMSE decreases and the coefficient of determination increases for most of the cases. In general, it has presented similar features as the hourly comparison, showing a reasonable agreement in warm climate regions for all seasons and in cold regions during warm seasons. However, significant underestimations can still be observed during the winter at Sioux Falls station.

A similar seasonal comparison of hourly insolation is presented in Fig. 6. The pyranometer data come from USCRN La Junta and Nunn stations in Colorado. La Junta is located in southeastern Colorado, while Nunn is

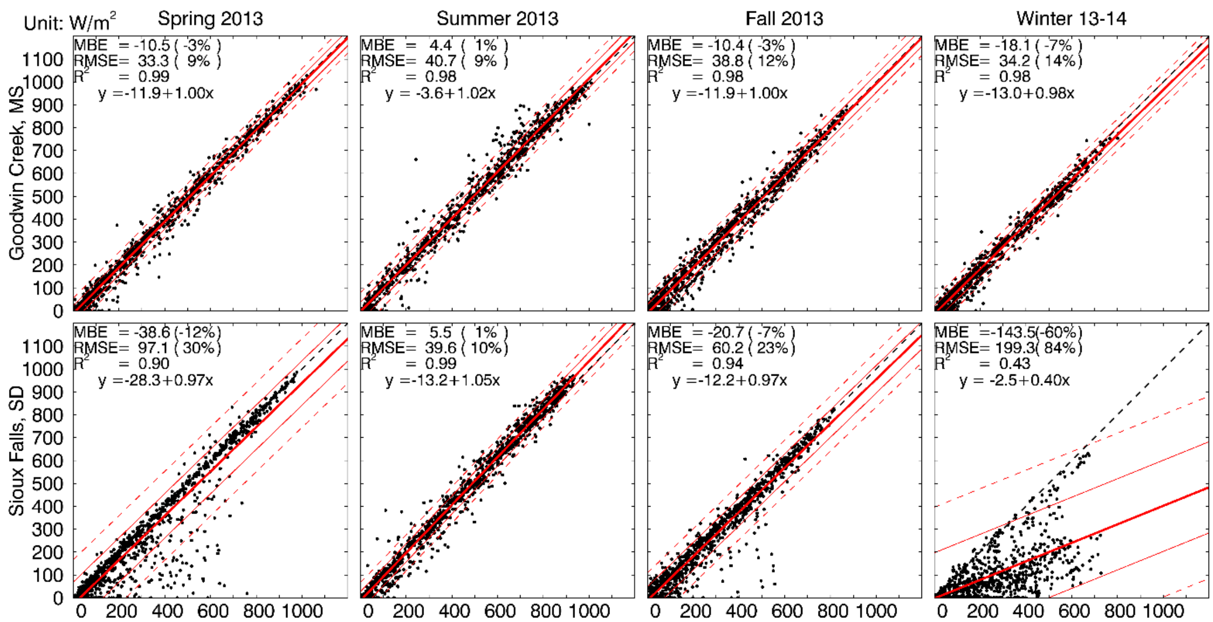

Fig. 4. Seasonal comparison of hourly insolation (W/m^2) estimated from GOES-East Images (along y-axis of each panel) and measured from SURFRAD stations (along x-axis of each panel) at Goodwin Creek, MS (top panels) and Sioux Falls, SD (bottom panels). Seasons are indicated at the top. Statistics and linear regression equations are indicated in the top-left corner of each panel. The black dashed lines are 1:1 lines; red bold lines are the best-fit lines; red solid lines and dashed lines show ranges of ±1σ and ±2σ deviation.

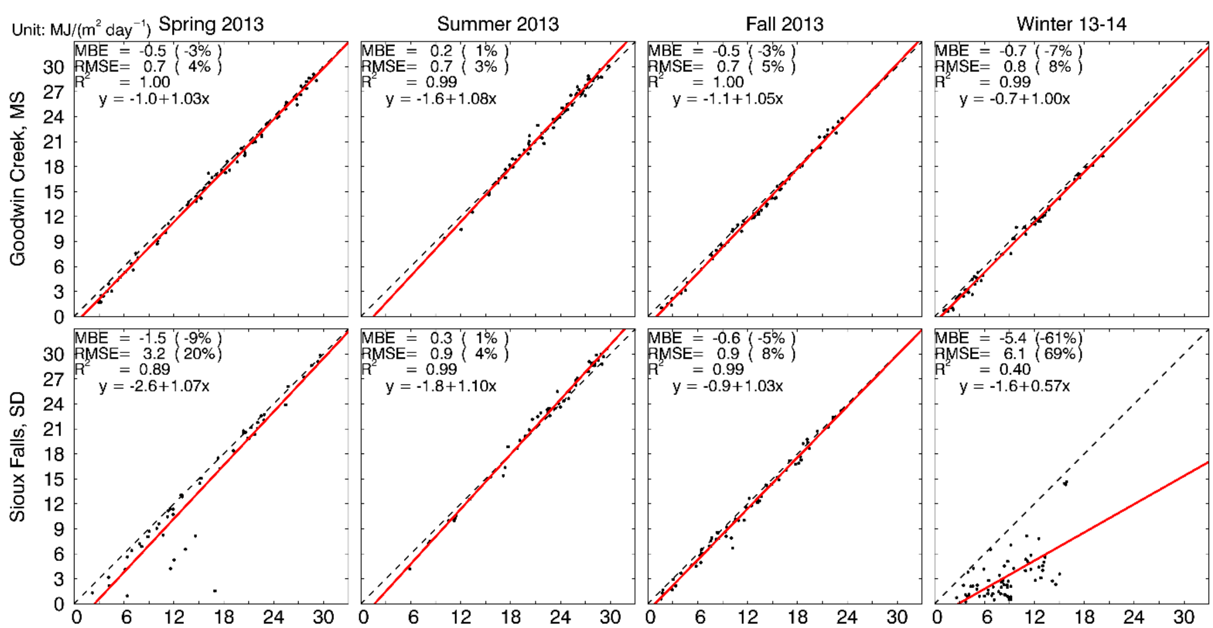

Fig. 5. Same as Fig. 4, except for daily cumulative insolation (MJ/m^2/day).

near the northern boundary. Since they both located to the east of the Rocky Mountains, they should have similar climates, although Nunn is supposed to be colder than La Junta because of the latitude difference.

The scatter plots have indicated: 1) the satellite retrieval can provide a reasonable estimation of insolation with respect to USCRN measurements during the summer and fall of year 2013; 2) spring estimation was not too bad, although we found decreases in R^2 values, and RMSE values were above 20% of the mean; 3) underestimations were still obvious for the winter, which was indicated by large negative MBE and relative low R^2.

Generally, winter UAH insolation retrieval has shown similar underestimation features with respect to the observations from some USCRN and SURFRAD stations. It was hypothesized that such underestimation is mainly due to snow cover at the beginning. To test our hypothesis, a snow filtering system based on pyranometer network measurements (precipitation and surface temperature) and MODIS snow cover product, was applied

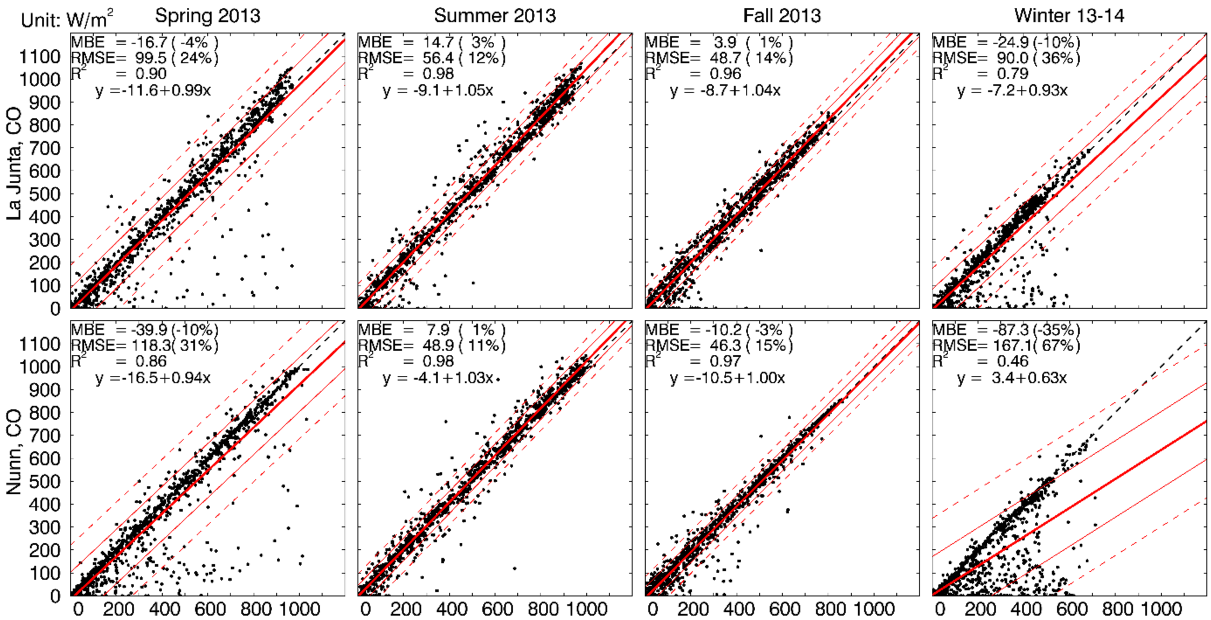

Fig. 6. Same as Fig. 4, except for USCRN La Junta, CO (top panels) and Nunn, CO (bottom panels).

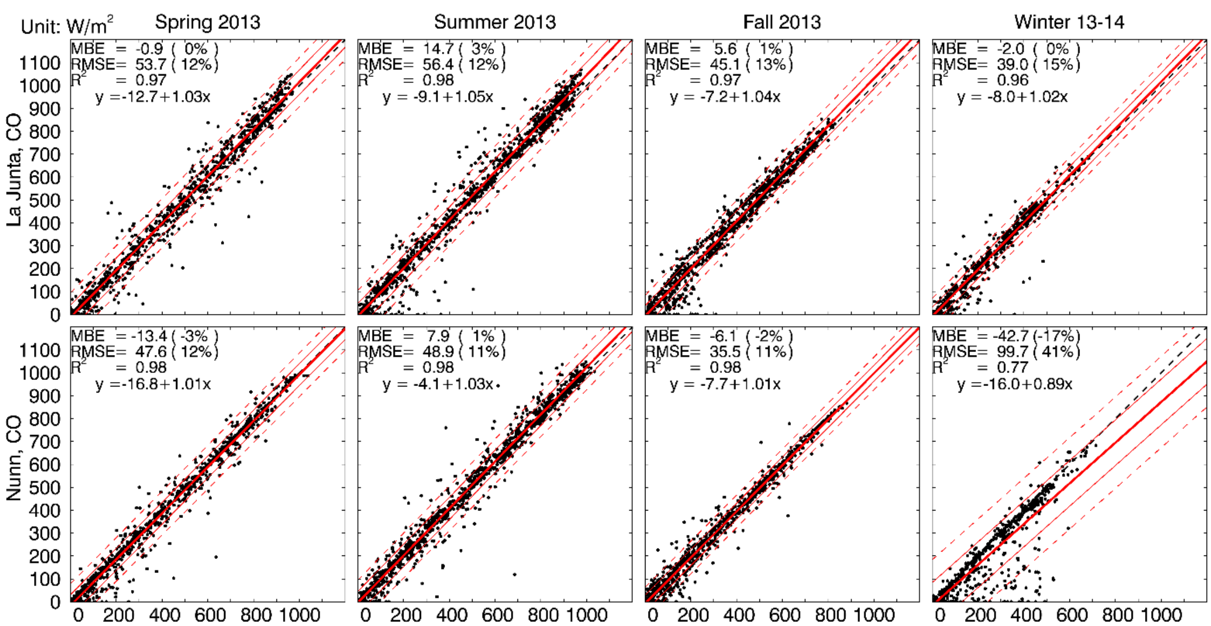

Fig. 7. Same as Fig. 6, except that a snow filtering algorithm (based on USCRN measurements and MODIS snow cover product) is applied to get rid of snow covered cases.

for all seasons except summer. Results after filtering the snow cases for USCRN La Junta, CO and Nunn, CO sites are presented in Fig. 7. Improvements, in terms of decreases in MBE and RMSE values, and increases in R^2 values, have been clearly shown for all cases. The algorithm works well for both sites during the spring and fall, and for La Junta site during the winter; however, the underestimation features have not been completely removed for Nunn site during the winter. Failures in attempting to eliminate snow cover effects have also been observed for some other stations, most of which are in the Northern U.S.

The failure of snow filtering implied the snow cover effects may not be the only cause of systematic bias. To find out other possible causes of wintertime underestimation, a detailed investigation of UAH archived products has been conducted. A set of archived products including the insolation, cloud albedo, longwave infrared temperature and surface albedo products at 18:45 UTC on 11 January 2014 is shown in Fig. 8.

We can find that the insolation product (Fig. 8a) coincided with cloud albedo map (Fig.8b), since a larger cloud albedo implies more energy reflection, which will reduce the amount of radiation reaching the Earth's surface. However, the cloud albedo map seems unreason-

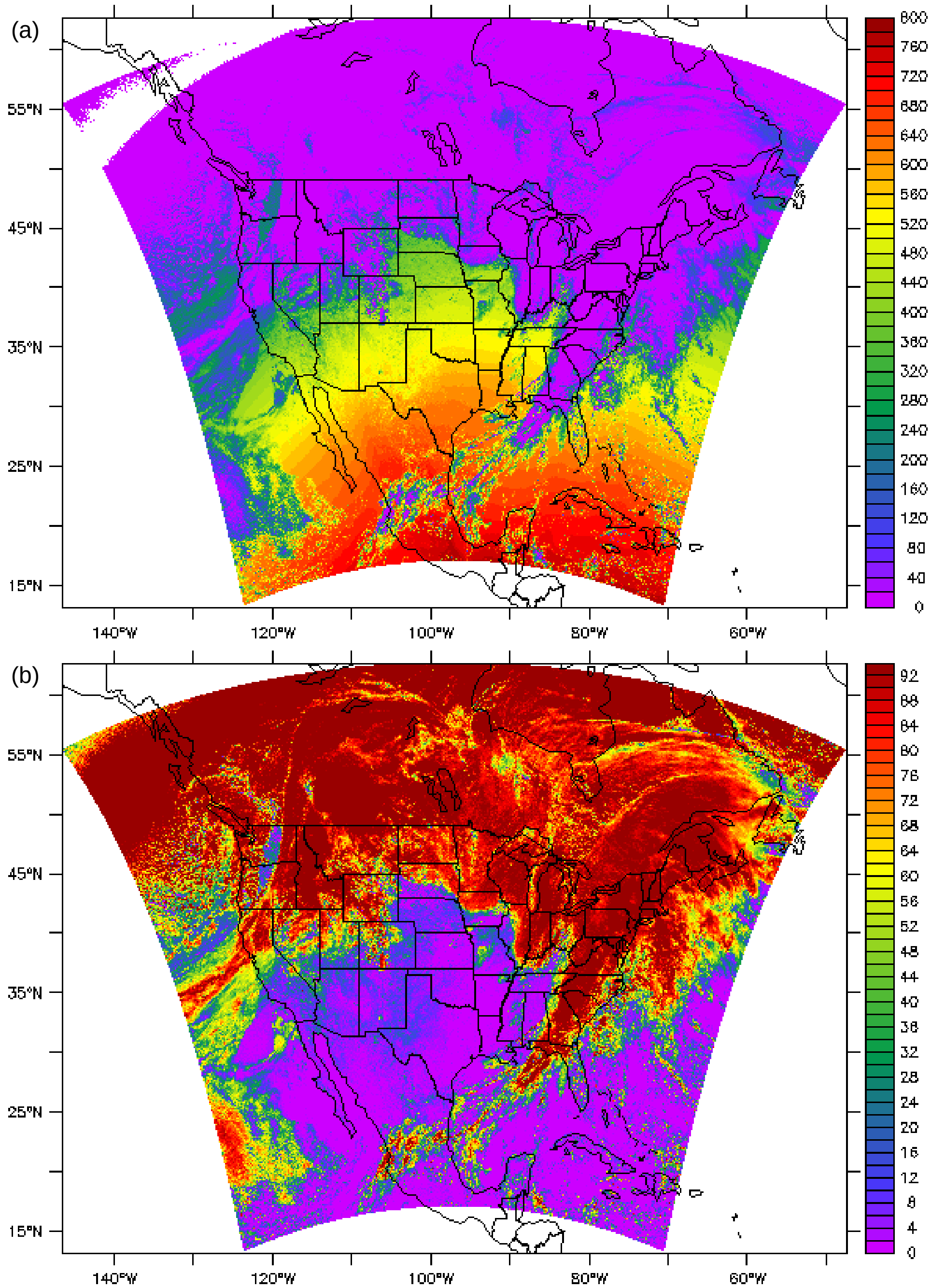

Fig. 8. UAH archived products of a) insolation (W/m^2), b) cloud albedo (%), c) longwave infrared temperature (K), and d) surface albedo (%) at 18:45 UTC on 11 January 2014.

able in some regions when compared with the longwave infrared temperature (LWIR) plot (Fig. 8c). Some north-central states have LWIR values between 260K and 270K. This temperature range may not only come from low-level clouds, but the cold surface, since this region can be extremely cold during the winter with snow covered surface (represented by high surface albedo, see Fig. 8d). Therefore, the GPGS system may not be able to distinguish clouds from the surface via visible-band images only, when some dark clouds appear above a bright surface persistent snow.

Meanwhile, Fig. 8 has indicated another issue within the retrieval system that areas with high surface albedo were located not only in the continent of North America, but also part of the Pacific Ocean. The cause is still unclear and requires further investigation on the algorithm.

7. CONCLUSIONS

Results have shown that the UAH insolation product compares well with pyranometer measurements under clear-sky conditions; but when sky is cloudy, the spatial

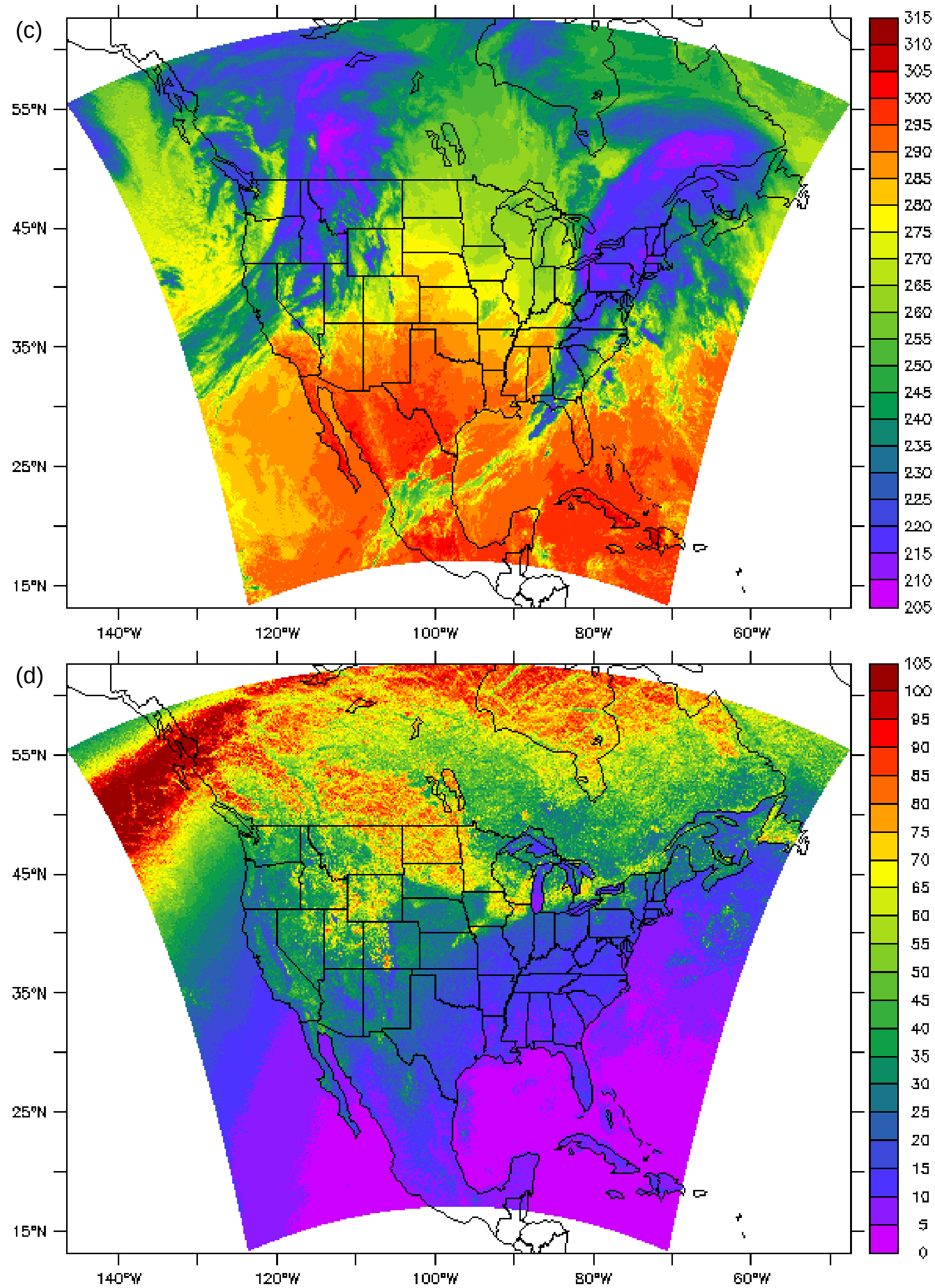

Fig. 8. (*continued*)

scale and transient nature of clouds makes the comparison difficult. Other sources of uncertainties include discrepancies in instrument working principles, pyranometer calibration, dust or insects above pyranometer sensor, satellite sensor degradation, navigation error, etc.

In regions with warm climate, the insolation retrieval has shown a reasonable agreement compared to pyranometer measurements for all seasons. However, significant underestimations were presented in cold climate regions during the cold seasons. To test if such bias came from the effects of snow cover, a snow filtering algorithm was applied to eliminate the snow effects based on USCRN measurements and MODIS snow cover product. However, only part of stations (mainly in the warmer regions) have shown improvements as we expected.

One guess for the failure of snow filtering is that the minimum brightness detection module in the retrieval system has failed when clouds appeared above a bright surface covered by persistent snow, which was implied by a comprehensive investigation of the UAH archived products. Moreover, another issue in surface albedo estimation over the ocean was noticed while the cause is still unclear and requires further investigation.

Acknowledgments. The findings presented here were accomplished under partial support from NASA Science Mission Directorate Applied Sciences Program. Note the results in this study do not necessarily reflect policy or science positions by the funding agencies.

REFERENCES

Ali, M. H., and I. Abustan, 2014: NATURAL RESOURCES AND DEVELOPMENT A new novel index for evaluating model performance . *J. Nat. Resour. Dev.*, **4**, 1–9, doi:10.5027/jnrd.v4i0.01.

Augustine, J. A., J. J. DeLuisi, and C. N. Long, 2000: SURFRAD—A National Surface Radiation Budget Network for Atmospheric Research. *Bull. Am. Meteorol. Soc.*, **81**, 2341–2357, doi:10.1175/1520-0477(2000)081<2341:SANSRB>2.3.CO;2. http://journals.ametsoc.org/doi/abs/10.1175/1520-0477%282000%29081%3C2341%3ASANSRB%3E2.3.CO%3B2.

——, G. B. Hodges, C. R. Cornwall, J. J. Michalsky, and C. I. Medina, 2005: An Update on SURFRAD—The GCOS Surface Radiation Budget Network for the Continental United States. *J. Atmos. Ocean. Technol.*, **22**, 1460–1472, doi:10.1175/JTECH1806.1. http://www.scopus.com/inward/record.url?eid=2-s2.0-27744593779&partnerID=tZOtx3y1.

Benjamin, S. G., and Coauthors, 2016: A North American Hourly Assimilation and Model Forecast Cycle: The Rapid Refresh. *Mon. Weather Rev.*, **144**, 1669–1694, doi:10.1175/MWR-D-15-0242.1. http://journals.ametsoc.org/doi/10.1175/MWR-D-15-0242.1.

Coulson, K. L., 1959: Characteristics of the radiation emerging from the top of a Rayleigh atmosphere—II. *Planet. Space Sci.*, **1**, 277–284, doi:10.1016/0032-0633(59)90032-7. http://linkinghub.elsevier.com/retrieve/pii/0032063359900327.

Diak, G. R., 2017: Investigations of improvements to an operational GOES-satellite-data-based insolation system using pyranometer data from the U.S. Climate Reference Network (USCRN). *Remote Sens. Environ.*, **195**, 79–95, doi:10.1016/j.rse.2017.04.002. http://dx.doi.org/10.1016/j.rse.2017.04.002.

Diak, G. R., and C. Gautier, 1983: Improvements to a Simple Physical Model for Estimating Insolation from GOES Data. *Am. Meteorol. Soc.*, **22**, 505–508, doi:10.1175/1520-0450(1983)022<0505:ITASPM>2.0.CO;2.

Diak, G. R., J. R. Mecikalski, M. C. Anderson, J. M. Norman, W. P. Kustas, R. D. Torn, and R. L. DeWolf, 2004: Estimating Land Surface Energy Budgets From Space: Review and Current Efforts at the University of Wisconsin—Madison and USDA–ARS. *Bull. Am. Meteorol. Soc.*, **85**, 65–78, doi:10.1175/BAMS-85-1-65. https://doi.org/10.1175/BAMS-85-1-65.

Diamond, H. J., and Coauthors, 2013: U.S. climate reference network after one decade of operations status and assessment. *Bull. Am. Meteorol. Soc.*, **94**, 485–498, doi:10.1175/BAMS-D-12-00170.1.

Gautier, C., G. Diak, and S. Masse, 1980: A simple physical model to estimate incident solar radiation at the surface from GOES satellite data. *J. Appl. Meteorol. Climatol.*, **19**, 1005–1012, doi:10.1175/1520-0450(1980)019<1005:ASPMTE>2.0.CO;2.

Habte, A., M. Sengupta, and S. Wilcox, 2012: Surface radiation from GOES: A physical approach. *27th Eur. Photovolt. Sol. Energy Conf. Exhib.*, 3052–3059.

Habte, A., M. Sengupta, and S. Wilcox, 2013: Validation of GOES-Derived Surface Radiation Using NOAA ’ s Physical Retrieval Method.

Haines, S. L., R. J. Suggs, and G. J. Jedlovec, 2004: The Geostationary Operational Environmental Satellite (GOES) product generation system. *NASA Tech. Memo., NASA TM-2004-213286*,. http://hdl.handle.net/2060/20050019524.

Jacobs, J. M., D. A. Myers, M. C. Anderson, and G. R. Diak, 2002: GOES surface insolation to estimate wetlands evapotranspiration. *J. Hydrol.*, **266**, 53–65, doi:10.1016/S0022-1694(02)00117-8.

Lacis, A. A., and J. E. Hansen, 1974: A Parameterization for Absorption of Solar Radiation in the Earth’s Atmosphere. *J. Atmos. Sci.*, **31**, 118–133, doi:10.1175/1520-0469(1974)031<0118:APFTAO>2.0.CO;2.

Li, Z., C. H. Whitlock, and T. P. Charlock, 1995: Assessment of the Global Monthly Mean Surface Insolation Estimated from Satellite Measurements Using Global Energy Balance Archive Data. *J. Clim.*, **8**, 315–328, doi:10.1175/1520-0442(1995)008<0315:AOTGMM>2.0.CO;2. https://doi.org/10.1175/1520-0442(1995)008%3C0315:AOTGMM%3E2.0.CO.

Mecikalski, J. R., D. M. Sumner, J. M. Jacobs, C. S. Pathak, S. J. Paech, and E. M. Douglas, 2011: Use of Visible Geostationary Operational Meteorological Satellite Imagery in Mapping Reference and Potential Evapotranspiration over Florida. *Evapotranspiration*, 446, doi:10.5772/585. http://www.intechopen.com/books/evapotranspiration/.

Mesinger, F., and Coauthors, 2006: North American regional reanalysis. *Bull. Am. Meteorol. Soc.*, **87**, 343–360, doi:10.1175/BAMS-87-3-343.

Otkin, J. a, M. C. Anderson, J. R. Mecikalski, and G. R. Diak, 2005: Validation of GOES-Based Insolation Estimates Using Data from the U.S. Climate Reference Network. *J. Hydrometeorol.*, **6**, 460–475, doi:10.1175/JHM440.1. http://journals.ametsoc.org/doi/abs/10.1175/JHM440.1.

Paltridge, G. W., 1973: Direct Measurement of Water Vapor Absorption of Solar Radiation in the Free Atmosphere. *J. Atmos. Sci.*, **30**, 156–160, doi:10.1175/1520-0469(1973)030<0156:DMOWVA>2.0.CO;2. http://journals.ametsoc.org/doi/abs/10.1175/1520-0469%281973%29030%3C0156%3ADMOWVA%

3E2.0.CO%3B2.

Pinker, R. T., R. Frouin, and Z. Li, 1995: A review of satellite methods to derive surface shortwave irradiance. *Remote Sens. Environ.*, **51**, 108–124, doi:10.1016/0034-4257(94)00069-Y.

Podlasly, C., and F. H. Berger, 2002: Insolation estimates for the LITFASS area derived from high resolution satellite data. *Theor. Appl. Climatol.*, **73**, 87–95, doi:10.1007/s00704-002-0695-3. http://link.springer.com/10.1007/s00704-002-0695-3.

Schmetz, J., 1989: Towards a surface radiation climatology: Retrieval of downward irradiances from satellites. *Atmos. Res.*, **23**, 287–321, doi:10.1016/0169-8095(89)90023-9.

Simon, H., K. R. Baker, and S. Phillips, 2012: Compilation and interpretation of photochemical model performance statistics published between 2006 and 2012. *Atmos. Environ.*, **61**, 124–139, doi:10.1016/j.atmosenv.2012.07.012. http://dx.doi.org/10.1016/j.atmosenv.2012.07.012.

Tarpley, J. D., 1979: Estimating Incident Solar Radiation at the Surface from Geostationary Satellite Data. *J. Appl. Meteorol.*, **18**, 1172–1181, doi:10.1175/1520-0450(1979)018<1172:EISRAT>2.0.CO;2. http://dx.doi.org/10.1175/1520-0450(1979)018%3C1172:EISRAT%3E2.0.CO.